Contribution of Atmospheric Rivers to Antarctic Precipitation

Jan T. M. Lenaerts[1,*], Michelle L. Maclennan[1,*], Christine Shields[2], Jonathan D. Wille[3]

[1]Department of Atmospheric and Oceanic Sciences, University of Colorado Boulder, Boulder CO, USA
[2]National Center for Atmospheric Research, Boulder CO, USA
[3]Institut des Géosciences de l'Environnement, Grenoble, France
* These authors have contributed equally to the work

Key Points:

- Atmospheric rivers (ARs) contribute around 13±3% to Antarctic Ice Sheet (AIS) precipitation.
- The relative contribution of ARs to precipitation is most substantial in East Antarctica.
- ARs explain a large fraction (35%) of interannual variability in AIS precipitation.

Corresponding author: Jan T. M. Lenaerts, Jan.Lenaerts@colorado.edu

Abstract

Atmospheric rivers (ARs) are efficient mechanisms for transporting atmospheric moisture from low latitudes to the Antarctic Ice Sheet (AIS). While AR events occur infrequently, they can lead to extreme precipitation and surface melt events on the AIS. Here we estimate the contribution of ARs to total Antarctic precipitation, by combining precipitation from atmospheric reanalyses and an polar-specific AR detection algorithm. We show that ARs contribute substantially to Antarctic precipitation, especially on East Antarctica at elevations below 3000 meters. ARs play a vital role in explaining the substantial year-to-year variability in Antarctic precipitation. Our results highlight that ARs are an important component for understanding present and future Antarctic mass balance trends and variability.

Plain Language Summary

Antarctica is the driest continent on Earth. The rare snowfall events on the cold Antarctic desert usually come from so-called atmospheric rivers, the same type of systems that bring winter precipitation along the western coasts of the American continents, such as the Pacific Northwest in the United States. Here we estimate how much precipitation on Antarctica is associated with these atmospheric rivers. Even though they only occur a few days per year, atmospheric rivers explain around 13% of the total Antarctic precipitation. Even more importantly, we find a strong link between year-to-year variations in Antarctic precipitation and atmospheric rivers, underlining the importance of these systems for understanding current and future changes of the Antarctic ice sheet contribution to global sea level rise.

1 Introduction

The Antarctic Ice Sheet (AIS) is losing mass at an accelerated pace, with a tripling of mass loss (200 Gt yr^{-1} or Gigatonnes (10^{12} kg) per year) in recent years (2012-2017) relative to the early 1990s (Shepherd et al., 2018; Rignot et al., 2019). On top of that multi-decadal AIS mass loss signal, which is primarily driven by ocean warming and subsequent ice shelf thinning and areal loss, and grounding line retreat, AIS mass balance varies substantially from year to year (Wouters et al., 2013; Rignot et al., 2019). These mass balance variations are determined by atmospheric processes, particularly snowfall, which is the primary input term of the AIS mass balance (Lenaerts et al., 2019). While

annual snowfall rates on AIS are generally low (<200 mm per year), a substantial portion of the annual snowfall is associated with highly episodic marine air intrusions (Nicolas et al., 2011; Maclennan & Lenaerts, 2021) or synoptic-scale cyclones (Dalaiden et al., 2020; Turner et al., 2019). Some of these systems generate long, narrow plumes of strong horizontal water vapor transport, referred to as atmospheric rivers (ARs; Zhu & Newell, 1998). While ARs are well known to impact certain mid-latitude regions, particularly the west coast of the American continents, recent work has highlighted their importance for ice sheet mass balance. For example, Mattingly et al. (2020) showed that atmospheric rivers in summer enhance surface melt and rainfall over the Greenland Ice Sheet. Wille et al. (2019) demonstrated that most surface melt events on the West Antarctic Ice Sheet are explained by ARs, as they bring relatively warm air masses from lower latitudes, sometimes as far as the subtropics (Terpstra et al., 2021). As surface melt and rain on the AIS is generally limited to the ice shelves (Trusel et al., 2013; Johnson et al., 2021), and nearly all meltwater refreezes in the firn, ARs are currently more relevant for precipitation on the AIS. Considering that AR are likely to become more impactful in the future (Payne et al., 2020), and AIS precipitation is expected to increase (Dalaiden et al., 2020; Lenaerts et al., 2016), it is essential to better constrain ARs and their impact on contemporary AIS surface mass balance. In situ observations on the East Antarctic escarpment have shown that ARs can contribute up to 80% of the annual snowfall (Gorodetskaya et al., 2014). In West Antarctica, seasonal surface height increases, as measured by satellite laser altimetry, can be attributed to unusually strong AR activity (Adusumilli et al., 2021). Most recently, Wille et al. (2021) used an AR detection algorithm to confirm that, while ARs only occur a few times per year along the Antarctic coastline, they contribute significantly to AIS snowfall especially in East Antarctica. A question that emerges from this previous work, in the framework of ongoing AIS mass loss, is: how much mass, in the form of precipitation, do ARs contribute to the AIS every year? Here we aim to address that question, using a combination of a polar-specific AR algorithm and reanalysis precipitation products. Section 2 discusses the data and methods used in this study. Section 3 presents the results, and Section 4 provides a discussion of our findings and conclusions.

2 Data and Methods

2.1 MERRA-2

In this work, we use output of the atmospheric reanalysis product MERRA-2 (Gelaro et al., 2017) from the National Aeronautics and Space Association (NASA). In particular, we use total (snowfall + rainfall) precipitation fields at three-hourly (for the AR precipitation, see below) and monthly time resolution (for the total). We included rainfall in our study, since it is very small over Antarctica (Vignon et al., 2021), and most rain water instantaneously refreezes in the cold firn, essentially implying that rainfall is an input term of the current Antarctic mass balance. Effects of rain on firn thermal and density structure are not accounted for in this study. MERRA-2 is selected because the snow accumulation (i.e. precipitation - sublimation) field over Antarctica compares most favorably to ice core accumulation records of multiple state-of-the-art reanalysis products (Medley & Thomas, 2019).

2.2 AR detection algorithm

To detect atmospheric rivers, we use the detection algorithm described in Wille et al. (2021), which uses the meridional component of the integrated water vapor transport (vIVT) fields between 37.5°S and 80°S from the MERRA-2 atmospheric reanalysis. ARs are delineated by anomalously high (>98th percentile) vIVT values, and redetermined every 3 hours. If a filament of anomalously high vIVT values extends continuously for at least 20° in the meridional direction, then it is identified as an AR. It is a participating algorithm in ARTMIP (Atmospheric River Tracking Method Intercomparison Project; (Shields et al., 2018; Rutz et al., 2019)) and differs from many ARDTs in that is is regionally specific to Antarctica, not a generalized global algorithm, and detects ARs at a lower frequency compared to other global algorithms. Following Wille et al. (2021), we use vIVT instead of integrated water vapor (IWV) for AR precipitation attribution, given that the meridional moisture transport better reflects the dynamical processes associated to ARs. The algorithm excludes areas south of 80°S, since the AR vIVT signal quickly dissipates in the high-elevation interior of Antarctica as the humidity of the boundary layer is often dominated by the katabatic flow (Gorodetskaya et al., 2014).

Next, we combine this AR detection catalogue with MERRA-2 snowfall, and we define AR associated precipitation as precipitation that falls directly within each AR foot-

print, as well as in the 24-hour (± 6 hours) long period after an AR has made passage. This 24 ± 6 hour period, which is also used in Wille et al. (2021) is selected after careful analysis of precipitation rates in MERRA-2 during and after AR passage across the AIS for year 2019 (Figure 1). For this analysis, we used an hourly version of the AR detection algorithm (Alison Collow, personal communication), which provides more temporal detail but uses the same vIVT threshold method compared to the original 3-hourly algorithm (see above). We focus on the time period after the last time step an AR was detected, so we did not account for those time steps after which an AR was still detected. This gives insight in how precipitation rates vary after AR passage, or, in other words, how long ARs continue to affect precipitation after they have passed by a certain location. The results are summarized for the entire AIS and per glacier drainage basin (Figure 1), and show that precipitation rates quickly decline in the first ∼10 hours after AR passage, after which they the rate decline slows down. After 10 hours, precipitation rates have decreased to approximately half of the original, and after 20 hours to less than 40%. We decided to use 24 hours as a cut-off time, i.e. all precipitation before that time is considered AR precipitation, while any precipitation after 24 hours is not. We chose for this because of two main reasons: (1) at around 24 hours, more than 80% of cumulative precipitation has fallen since AR passage on average, and rates are decreasing only very slowly afterwards; (2) 24 hours is available in the 3-hourly AR catalogues we use in this study, and is transferable to studies for which only daily precipitation rates are available. To quantify the uncertainty associated to this choice, we use the standard deviation of the time step when 80% cumulative precipitation is reached in each glacier drainage basin (Figure 1), which equals ∼6 hours.

Next, we checked the validity of our choice with a slightly different approach, and using our original 3-hourly AR algorithm. We calculated the relative change in AIS-integrated AR precipitation with each 3-hourly increase in cut-off time (e.g. 3 hours only accounts for precipitation until 3 hours after passage to the AR precipitation). While the relative increase initially increases steeply (e.g. 18% increase when using 6 hrs past AR passage compared to using 3 hrs past AR passage), the relative increase between each 3 hr increase quickly lowers, and is lower than 5% after 18 hours. This remaining small increase with a later cut-off time is to be expected, and likely due to the residual AR-related moisture being incorporated in mesoscale cyclogenesis over the AIS, the impact of a new AR as part of a series of ARs passing by the same location, and/or the general occur-

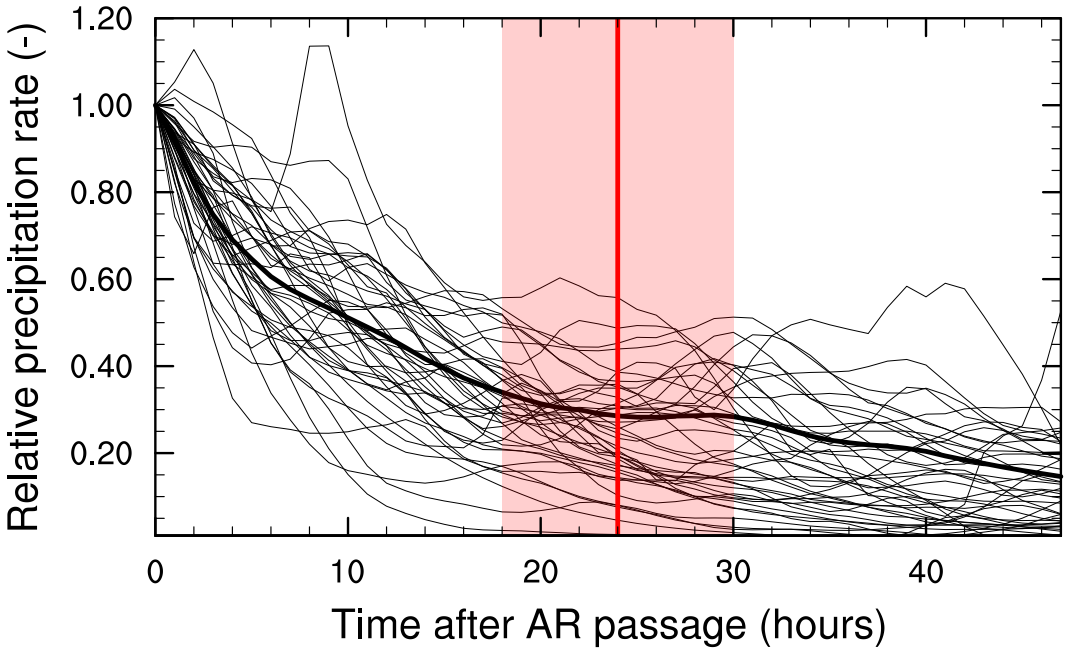

Figure 1. Mean precipitation rate as a function of time after AR passage, expressed relative to the last time step of AR passage, on the AIS for the year 2019. The thick black line denotes the mean of all ARs on the AIS, and the thin black lines show results for each individual glacier drainage basins (Shepherd et al., 2012). The vertical red line and shading show the 24 ± 6 hr time window that we have selected as the most suitable period to present our AR precipitation results.

rence of AIS precipitation occurring outside the footprint of the detected ARs. This finding validates our choice of 24 ± 6 hour period, which likely includes most of the AR attributed precipitation while excluding most precipitation from other sources.

3 Results

First we focus our analysis on the AIS-wide impact of ARs to precipitation. The annual precipitation that can be attributed to ARs varies from less than 1 mm w.e. per year on the Antarctic Plateau to >100 mm w.e. per year on the low-elevation coastal zones (Figure 3a). While total annual precipitation exhibits a similar gradient, with high precipitation rates along the coast and very low precipitation rates in the interior (e.g. Lenaerts et al., 2019), the relative contribution of ARs to that total precipitation is generally highest at lower elevations of the grounded ice sheet. The highest contributions (>20 %) are found in large parts of East Antarctica (Figure 3b), while relative contri-

butions are lowest on the large Ross, Ronne-Filchner, and Amery ice shelves, and in the high-elevation (>3000 m a.s.l.) interior. Remarkably, the relative contribution of ARs is markedly lower in the entirety of West Antarctica (generally <10%) compared to East Antarctica. Integrated over the full ice sheet (including ice shelves, and excluding areas poleward of 80°S), the AR precipitation equals 336 ± 83 Gt yr^{-1}, equivalent to a 13±3% of total precipitation (which equals 2592±127 Gt yr^{-1}). The relative importance of AR precipitation is slightly higher on the grounded ice sheet (13%) than on ice shelves (11%), and higher on East Antarctica (16%) than on West Antarctica (9%) and the Antarctic Peninsula (10%). These results imply that the relative impact of ARs on precipitation is at least a magnitude higher than their frequency on the AIS, which does not exceed 1 to 1.5% (Wille et al., 2021).

Interannual variations in AR precipitation on the AIS are substantial, which is illustrated by the high (25%) ratio between the 1980-2019 AR precipitation standard deviation and mean, in comparison to the 5% ratio for total precipitation. This is further confirmed by the strong correlation (squared correlation coefficient $R^2 = 0.96$) between interannual variations of ice sheet integrated AR precipitation and its relative contribution to total AIS precipitation (Figure 3c). Detrended AIS AR precipitation and total precipitation are moderately correlated (linear slope = 0.98; $R^2 = 0.35$), indicating that ARs can explain more than a third of the interannual variability in total AIS precipitation, almost three times as much as ARs contribute to mean precipitation. Additionally, we find that the relative contribution of ARs to total AIS precipitation displays a small but discernible seasonal cycle (not shown), with a peak in winter and spring (>13.5%) and a relative minimum (<12.5%) in summer (Dec-Feb). Considering the substantial interannual variations, this seasonal cycle is nonetheless non-significant.

On top of these interannual variations, MERRA-2 suggests that total AIS precipitation has decreased during 1980-2019, albeit at a non-significant rate (-2.3±1.7 Gt yr^{-2} p=0.2). AR precipitation, on the other hand, shows a clear and statistically significant upward trend (2.5±1.1 Gt yr^{-2}, p=0.02). The opposite long-term trends imply that the relative contribution of ARs to AIS precipitation has increased towards the later years of the time period (Figure 3), and relative AR contribution has increased substantially (0.11±0.04 % yr^{-1}, p<0.01), both for the grounded ice sheet and ice shelves. In 2009 and 2011, when multiple ARs hit the Dronning Maud Land area (Gorodetskaya et al., 2014), the AR contribution exceeded 20%.

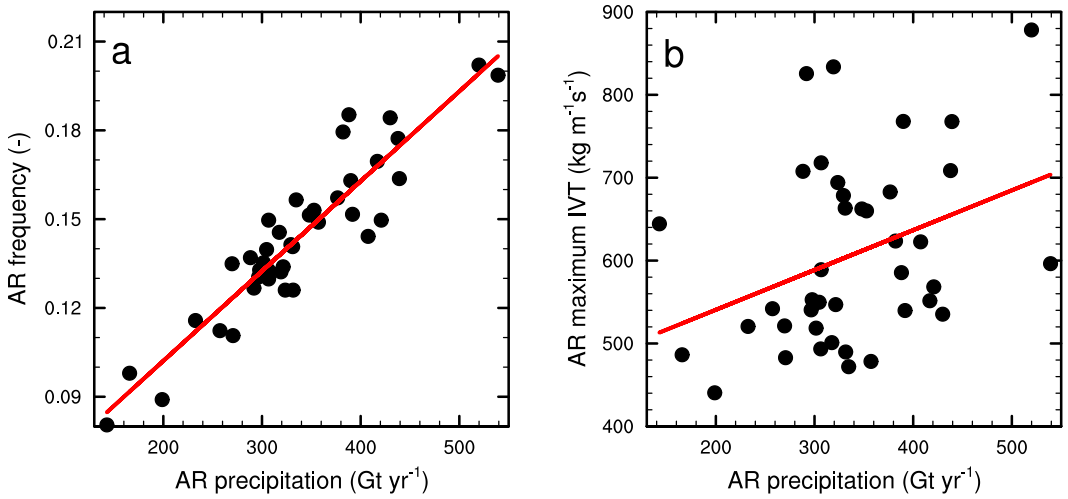

Figure 2. Annual AIS AR precipitation (1980-2019, horizontal axis) versus (a) annual AR frequency (1980-2019) on the AIS, defined here as the relative time an AR exists anywhere on the AIS; and (b) Annual mean (1980-2019) AR strength, approximated here by the mean IVT maximum found in all Antarctic ARs during each year.

An additional question emerging from our results is: what drives these variations in AR precipitation on the AIS? Both interannual variability and long-term trend in AR precipitation are strongly (R^2=0.85, p<0.01) correlated with the frequency of ARs on Antarctica (Figure 2), indicating that years with more (less) ARs making landfall on AIS are also associated with more (less) AR precipitation. However, we also find a small but significantly positive (R^2=0.13, p=0.02) correlation between AR precipitation and the annual average maximum IVT value in ARs on the AIS (Figure S1), suggesting a potential link between the strength of ARs (as measured by IVT) on Antarctica and their precipitation.

To further interpret the regional variability in the impact of ARs on Antarctic precipitation, we direct our analysis to individual glacier drainage basins. Figure 4a confirms that ARs contribute most to the total precipitation in the coastal East Antarctic basins (basins 5-9 and 12-15), with contributions of 12 up to 20% (basin 8). The coastal WAIS and interior EAIS basins show contributions of 10% and lower. Lowest AR contributions to precipitation are found on Ross shelf (<5 %), where AR frequency is also lowest, but summer ARs have been shown to induce surface melt (Wille et al., 2019). The spatial pattern in the extent to which ARs explain interannual variability (Figure

4b) largely reflects that of the AR contribution to the total, but the percentages are 3 to 4 times higher in most basins. In the coastal EAIS basins, 60-75% of the variability in total precipitation is explained by ARs. Averaged across the EAIS, the explained variance is 66%, substantially higher than the WAIS (55%) and the AP (34%).

While we found an overall positive trend in AR precipitation over the AIS, along with a small negative trend in total precipitation, these long term trends vary considerably from basin to basin (Figure 3c). In terms of total precipitation, we find strongly negative trends in Wilkes Land and western WAIS (basins 12 to 20), and overall positive or negligible trends in other regions. AR precipitation trends are positive in most basins, and only negative in the western Wilkes Land region (basins 12-13). We find qualitative agreement between the trend signs in most basins, suggesting that the long-term trends in AR precipitation partially explain the trends in total precipitation.

Finally, it is known that ARs, in part because of their remote, relatively warm source region and strong energetics, are able to penetrate deep in the interior of the ice sheet. We can validate this hypothesis using our results, as summarized in Figure 5. While the absolute precipitation rates associated to ARs clearly drop with elevation and distance to the coast (Figure 3a), their relative contribution to total precipitation remains remarkably constant from the coast all the way to 3000 meters a.s.l.,. Above that elevation, the AR contribution drops sharply, but the associated uncertainties are large given that we have no data poleward of 80°S. Similarly, the contribution to total precipitation variability remains constant from 0–3000 m a.s.l., and only slightly decreases above that elevation. This signal is pretty consistent among different basins, despite inter-basin differences in values, and indicates that ARs are equally relevant to explaining annual accumulation and its interannual variability in many interior, dry areas below 3000 m a.s.l., where many ice cores are taken, compared to a low-elevation, maritime location.

4 Conclusions and Discussion

Our study combines an polar-specific AR detection algorithm with MERRA-2 precipitation rates to quantify the contribution of ARs to Antarctic snowfall. We find that, integrated over the ice sheet, ARs contribute around 13% to Antarctic snowfall. The contribution varies substantially from year to year and on a regional (glacier basin) scale, but is relatively constant throughout the seasons and across elevation.

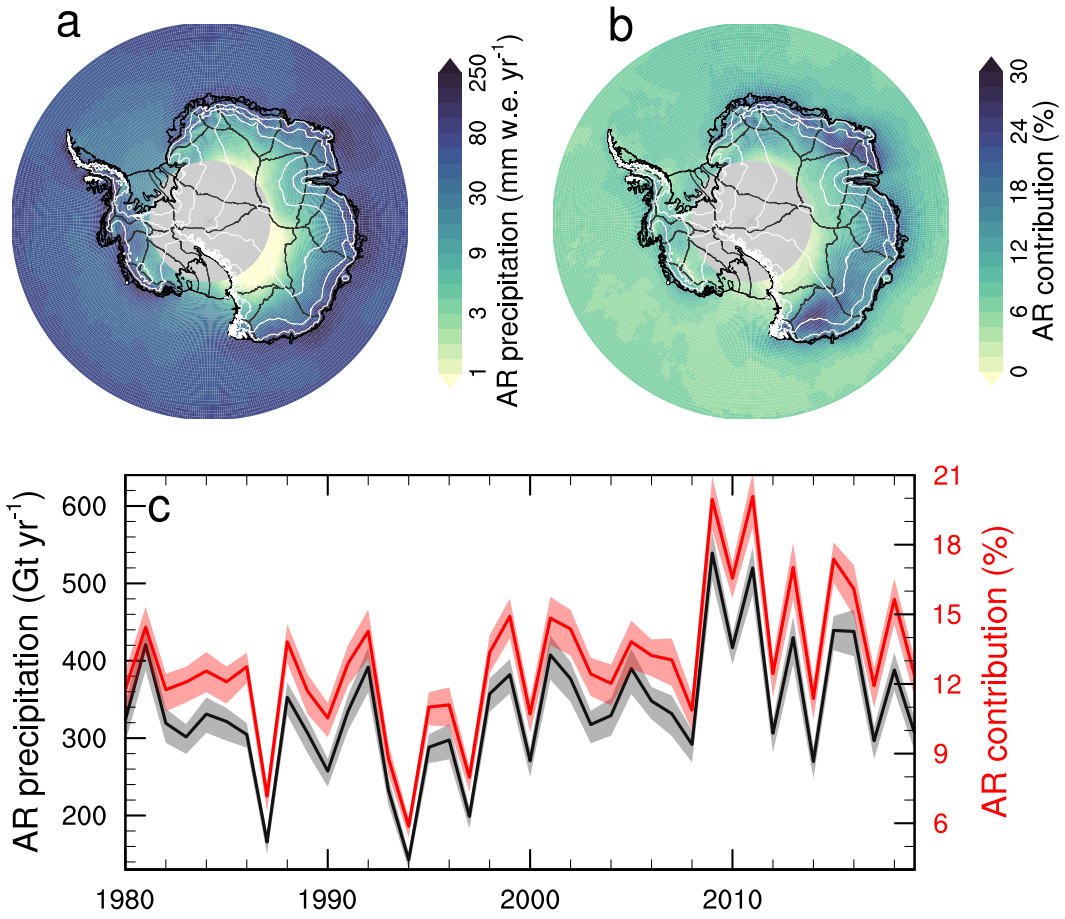

Figure 3. (a) 1980–2017 average precipitation attributed to ARs (mm w.e. per year); (b) 1980–2017 average relative contribution of AR precipitation (as shown in (a)) to the total annual precipitation; (c) Time series (1980-2017) of total AIS (grounded ice sheet and ice shelves) AR precipitation (black, in Gt yr^{-1}), and relative contribution of AR precipitation to total precipitation (in red, in %). The delineations of the drainage basins that are used further in this study are shown in thin black lines, and the grounding line and ice shelf boundaries are shown in thicker black lines.

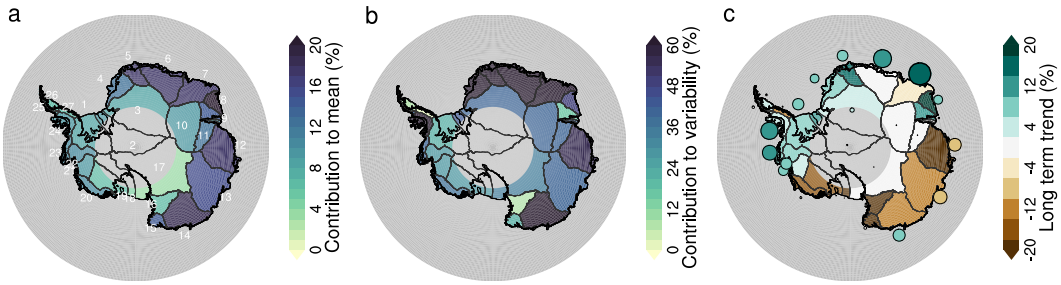

Figure 4. Relative contribution of AR precipitation to (a) the 1980–2019 average total precipitation; (b) the 1980–2017 interannual variability, defined as the percentage of explained variability of the best (positive) linear correlation between detrended annual AR and total precipitation; (c) the 1980–2019 relative change in total precipitation, with the dots showing relative change in AR precipitation (with same color scheme than total precipitation, and size proportional to relative change). Note that basins that are entirely poleward of 80°S are excluded in this analysis, but basins that partly cover >80°S only include those areas <80°S.

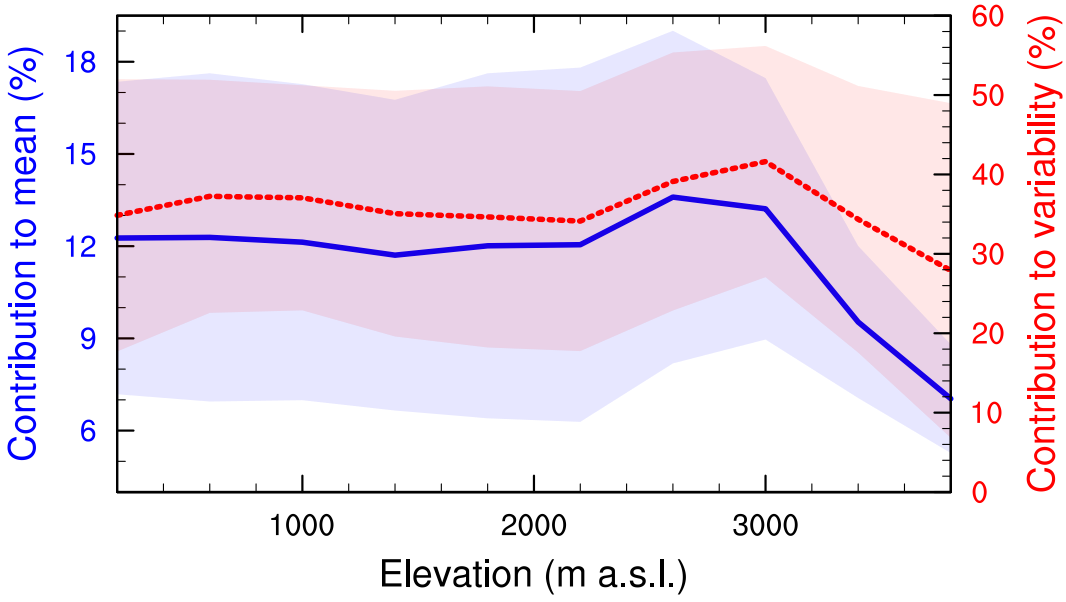

Figure 5. Relative contribution of AR precipitation to total precipitation (solid blue; left axis), and total precipitation variability (dashed red; right axis), as a function of elevation. The thick line shows the average of all basins, and the band indicates twice the standard deviation across all basins.

We acknowledge that substantial uncertainties are associated with our findings, particularly as a result of our choice of AR detection algorithm and precipitation dataset. On the other hand, we have several reasons to believe that our estimates are likely conservative. First of all, our precipitation product MERRA-2 is a global, gridded atmospheric reanalysis that does not assimilate but parameterizes precipitation rates and has a modest horizontal resolution (0.5 x 0.625 degrees). This likely leads to an underestimation of the highest precipitation rates, such as those associated to ARs, and thus an undercatch of the total precipitation assigned to an AR. Secondly, our assumed spatiotemporal footprint of an AR on precipitation likely underestimates its real footprint. We only assign precipitation directly underneath an AR to that system, while in reality, the precipitation field of an AR might be more expansive than that of the AR itself. The 24-hour time window after AR passage we use (and justify) might miss precipitation that persists for more than 24 hours after passage of strong AR systems (Wille et al., 2021). Thirdly, the AR detection algorithm used here is designed to capture high impact events, and likely misses weaker AR events more likely to be captured in global AR detection algorithms with lower thresholds. To further constrain ARs and their impact on Antarctica, future work should focus on using higher-resolution precipitation products (e.g. ERA5 reanalysis, regional climate models), in conjunction with varied AR detection algorithms applied to that same product to estimate uncertainty based on the detection method. In addition, AR detection algorithm can be refined, for example by categorizing AR strength based on AR structure, size, vIVT threshold, and/or other conditions.

Current AR impacts in most regions of Antarctica are focused on snowfall, and thus ARs contribute positively to Antarctic surface mass balance. However, larger contributions of ARs to snowfall in East Antarctica compared to West Antarctica suggest that that current AR impacts vary regionally. One hypothesis for this discrepancy is that West Antarctic ARs are less persistent, less meridionally expansive, and/or more of the 'windy and warm' rather than 'wet' type (Gonzales et al., 2020). Additionally, the zonal circulation around West Antarctica is better developed, and the position and strength of the Amundsen Sea Low, which is the dominant control of atmospheric circulation around West Antarctica (Turner et al., 2013), is extremely dynamic, both of which would limit the likelihood of the persistent atmospheric blocking needed for AR transport (Pohl et al., 2021). Further study is warranted to determine the AR flavors in different regions in Antarctica, and what impacts are associated to these different flavors. As global warm-

ing is likely to continue unabatedly in the future, leading to atmospheric temperature rise over Antarctica, AR strength and/or frequency might not only increase (Payne et al., 2020), but also their impact might shift. Particularly in the summer season and over coastal regions, ARs will bring enhanced potential of rainfall and surface melt at the expense of snowfall, which affects firn properties (Kuipers Munneke et al., 2014) and exacerbates the risk for ice slab formation, meltwater ponding, runoff, and ice shelf hydrofracture (Gilbert & Kittel, 2021). On the other hand, at higher elevations of the grounded ice sheet, ARs might bring even more enhanced snowfall in the future, aiding in mitigating ocean-driven Antarctic mass loss.

Acknowledgments

J. T. M. Lenaerts acknowledges support from NASA (grant 80NSSC20K0888) and the National Science foundation (NSF, award 1952199). This work is from the the TARSAN project, a component of the International Thwaites Glacier Collaboration (ITGC). Support from National Science Foundation (NSF: Grant 1929991) and Natural Environment Research Council (NERC: Grant NE/S006419/1). Logistics provided by NSF-U.S. Antarctic Program and NERC-British Antarctic Survey. ITGC Contribution No. ITGC-XXX. This material is based upon work supported by the U.S. Department of Energy, Office of Science, Office of Biological Environmental Research (BER), Regional and Global Model Analysis (RGMA) component of the Earth and Environmental System Modeling Program under Award Number DE-SC0022070 and NSF IA 1947282. This work was also supported by the National Center for Atmospheric Research (NCAR), which is a major facility sponsored by the NSF under Cooperative Agreement No. 1852977. C. Shields and M. Maclennan were partially supported under RGMA Award Number DE-SC0022070. M. L. Maclennan has also been supported by a NASA FINESST (grant 80NSSC21K1610). J. D. Wille acknowledges support from the Agence Nationale de la Recherche projects ANR-20-CE01-0013 (ARCA).

MERRA-2 precipitation data are available through the Goddard Earth Sciences Data and Information Services Center (hourly data at `https://disc.gsfc.nasa.gov/datasets/M2T1NXLFO_5.12.4/summary`, monthly means at `https://disc.gsfc.nasa.gov/datasets/M2TMNXLFO_5.12.4/summary`).

The ARTMIP catalogues are available on the NCAR CGD gateway via `https://doi.org/10.5065/D6R78D1M`. ARTMIP is a grass-roots community effort and includes

a collection of international researchers from universities, laboratories, and agencies. Co-chairs and committee members include Jonathan Rutz, Christine Shields, L. Ruby Leung, F. Martin Ralph, and Michael Wehner, Ashley Payne, Allison Collow, and Travis O'Brien. Details on catalogues developers can be found on the ARTMIP website. ARTMIP has received support from the US Department of Energy Office of Science Biological and Environmental Research (BER) as part of the Regional and Global Climate Modeling program, and the Center for Western Weather and Water Extremes (CW3E) at Scripps Institute for Oceanography at the University of California, San Diego.

References

Adusumilli, S., A. Fish, M., Fricker, H. A., & Medley, B. (2021, 3). Atmospheric River Precipitation Contributed to Rapid Increases in Surface Height of the West Antarctic Ice Sheet in 2019. *Geophysical Research Letters*, *48*(5), e2020GL091076. Retrieved from `https://doi.org/10.1029/2020GL091076` doi: 10.1029/2020GL091076

Dalaiden, Q., Goosse, H., Lenaerts, J. T. M., Cavitte, M. G. P., & Henderson, N. (2020). Future Antarctic snow accumulation trend is dominated by atmospheric synoptic-scale events. *Communications Earth & Environment*, *1*(1), 62. Retrieved from `https://doi.org/10.1038/s43247-020-00062-x` doi: 10.1038/s43247-020-00062-x

Gelaro, R., McCarty, W., Suárez, M. J., Todling, R., Molod, A., Takacs, L., ... Zhao, B. (2017, 5). The Modern-Era Retrospective Analysis for Research and Applications, Version 2 (MERRA-2). *Journal of Climate*, *30*(14), 5419–5454. Retrieved from `https://doi.org/10.1175/JCLI-D-16-0758.1` doi: 10.1175/JCLI-D-16-0758.1

Gilbert, E., & Kittel, C. (2021, 4). Surface Melt and Runoff on Antarctic Ice Shelves at 1.5°C, 2°C, and 4°C of Future Warming. *Geophysical Research Letters*, *48*(8), e2020GL091733. Retrieved from `https://doi.org/10.1029/2020GL091733` doi: 10.1029/2020GL091733

Gonzales, K. R., Swain, D. L., Barnes, E. A., & Diffenbaugh, N. S. (2020, 12). Moisture- Versus Wind-Dominated Flavors of Atmospheric Rivers. *Geophysical Research Letters*, *47*(23), e2020GL090042. Retrieved from `https://doi.org/10.1029/2020GL090042` doi: https://doi.org/10.1029/2020GL090042

Gorodetskaya, I. V., van Lipzig, N. P. M., Claes, K., Tsukernik, M., Ralph, F. M., Neff, W. D., ... van Lipzig, N. P. M. (2014, 9). The role of atmospheric rivers in anomalous snow accumulation in East Antarctica. *Geophysical Research Letters*, *41*(17), 6199–6206. Retrieved from http://doi.wiley.com/10.1002/2014GL060881 doi: 10.1002/2014GL060881

Johnson, A., Hock, R., & Fahnestock, M. (2021). Spatial variability and regional trends of Antarctic ice shelf surface melt duration over 1979–2020 derived from passive microwave data. *Journal of Glaciology*, 1–14. Retrieved from https://www.cambridge.org/core/article/spatial-variability-and-regional-trends-of-antarctic-ice-shelf-surface-melt-duration-over-19792020-derived-from-passive-microwave-data/65A10CC1A103D0BF9CE7F9A3C08180AB doi: 10.1017/jog.2021.112

Kuipers Munneke, P., M. Ligtenberg, S. R., van den Broeke, M. R., van Angelen, J. H., & Forster, R. R. (2014, 1). Explaining the presence of perennial liquid water bodies in the firn of the Greenland Ice Sheet. *Geophysical Research Letters*, *41*(2), 476–483. Retrieved from http://doi.wiley.com/10.1002/2013GL058389 doi: 10.1002/2013GL058389

Lenaerts, J. T. M., Medley, B., van den Broeke, M. R., & Wouters, B. (2019). Observing and Modeling Ice Sheet Surface Mass Balance. *Reviews of Geophysics*, *57*, 376–420. doi: 10.1029/2018RG000622

Lenaerts, J. T. M., Vizcaino, M., Fyke, J., van Kampenhout, L., & van den Broeke, M. (2016). Present-day and future Antarctic ice sheet climate and surface mass balance in the Community Earth System Model. *Climate Dynamics*, *47*(5-6), 1367–1381. doi: 10.1007/s00382-015-2907-4

Maclennan, M. L., & Lenaerts, J. T. (2021, 9). Large-Scale Atmospheric Drivers of Snowfall Over Thwaites Glacier, Antarctica. *Geophysical Research Letters*, *48*(17), e2021GL093644. Retrieved from https://doi.org/10.1029/2021GL093644 doi: 10.1029/2021GL093644

Mattingly, K. S., Mote, T. L., Fettweis, X., van As, D., Van Tricht, K., Lhermitte, S., ... Fausto, R. S. (2020). Strong Summer Atmospheric Rivers Trigger Greenland Ice Sheet Melt through Spatially Varying Surface Energy Balance and Cloud Regimes. *Journal of Climate*, *33*(16), 6809–6832. Retrieved from https://journals.ametsoc.org/view/journals/clim/33/

16/jcliD190835.xml doi: 10.1175/JCLI-D-19-0835.1

Medley, B., & Thomas, E. R. (2019). Increased snowfall over the Antarctic Ice Sheet mitigated twentieth-century sea-level rise. *Nature Climate Change*, *9*(1), 34–39. doi: 10.1038/s41558-018-0356-x

Nicolas, J. P., Bromwich, D. H., Nicolas, J. P., & Bromwich, D. H. (2011, 1). Climate of West Antarctica and Influence of Marine Air Intrusions*. *Journal of Climate*, *24*(1), 49–67. Retrieved from http://journals.ametsoc.org/doi/abs/10.1175/2010JCLI3522.1 doi: 10.1175/2010JCLI3522.1

Payne, A. E., Demory, M. E., Leung, L. R., Ramos, A. M., Shields, C. A., Rutz, J. J., ... Ralph, F. M. (2020). Responses and impacts of atmospheric rivers to climate change. *Nature Reviews Earth and Environment*, *1*(3), 143–157. Retrieved from https://doi.org/10.1038/s43017-020-0030-5 doi: 10.1038/s43017-020-0030-5

Pohl, B., Favier, V., Wille, J., Udy, D. G., Vance, T. R., Pergaud, J., ... Codron, F. (2021). Relationship Between Weather Regimes and Atmospheric Rivers in East Antarctica. *Journal of Geophysical Research: Atmospheres*, *126*(24), e2021JD035294. Retrieved from https://doi.org/10.1029/2021JD035294 doi: https://doi.org/10.1029/2021JD035294

Rignot, E., Mouginot, J., Scheuchl, B., van den Broeke, M., van Wessem, M. J., & Morlighem, M. (2019, 1). Four decades of Antarctic Ice Sheet mass balance from 1979–2017. *Proceedings of the National Academy of Sciences*, *116*(4), 1095 LP - 1103. Retrieved from http://www.pnas.org/content/116/4/1095.abstract doi: 10.1073/pnas.1812883116

Rutz, J. J., Shields, C. A., Lora, J. M., Payne, A. E., Guan, B., Ullrich, P., ... Viale, M. (2019, 12). The Atmospheric River Tracking Method Intercomparison Project (ARTMIP): Quantifying Uncertainties in Atmospheric River Climatology. *Journal of Geophysical Research: Atmospheres*, *124*(24), 13777–13802. Retrieved from https://doi.org/10.1029/2019JD030936 doi: 10.1029/2019JD030936

Shepherd, A., Ivins, E., Rignot, E., Smith, B., Van Den Broeke, M., Velicogna, I., ... Wouters, B. (2018, 6). Mass balance of the Antarctic Ice Sheet from 1992 to 2017. *Nature*, *558*(7709), 219–222. Retrieved from http://www.nature.com/articles/s41586-018-0179-yhttps://doi.org/10.1038/

s41586-018-0179-y doi: 10.1038/s41586-018-0179-y

Shepherd, A., Ivins, E. R., A, G., Barletta, V. R., Bentley, M. J., Bettadpur, S., ... Zwally, H. J. (2012). A Reconciled Estimate of Ice-Sheet Mass Balance. *Science*, *338*(6111), 1183–1189. doi: 10.1126/science.1228102

Shields, C. A., Rutz, J. J., Leung, L. Y., Martin Ralph, F., Wehner, M., Kawzenuk, B., ... Nguyen, P. (2018, 6). Atmospheric River Tracking Method Intercomparison Project (ARTMIP): Project goals and experimental design. *Geoscientific Model Development*, *11*(6), 2455–2474. Retrieved from https://gmd.copernicus.org/articles/11/2455/2018/https://gmd.copernicus.org/articles/11/2455/2018/gmd-11-2455-2018.pdf doi: 10.5194/gmd-11-2455-2018

Terpstra, A., Gorodetskaya, I. V., & Sodemann, H. (2021, 5). Linking Sub-Tropical Evaporation and Extreme Precipitation Over East Antarctica: An Atmospheric River Case Study. *Journal of Geophysical Research: Atmospheres*, *126*(9), e2020JD033617. Retrieved from https://doi.org/10.1029/2020JD033617 doi: https://doi.org/10.1029/2020JD033617

Trusel, L. D., Frey, K. E., Das, S. B., Munneke, P. K., & van den Broeke, M. R. (2013, 12). Satellite-based estimates of Antarctic surface meltwater fluxes. *Geophysical Research Letters*, *40*(23), 6148–6153. doi: 10.1002/2013GL058138

Turner, J., Bracegirdle, T. J., Phillips, T., Marshall, G. J., & Hosking, J. S. (2013, 3). An Initial Assessment of Antarctic Sea Ice Extent in the CMIP5 Models. *Journal of Climate*, *26*(5), 1473–1484. Retrieved from http://journals.ametsoc.org/doi/abs/10.1175/JCLI-D-12-00068.1 doi: 10.1175/JCLI-D-12-00068.1

Turner, J., Phillips, T., Thamban, M., Rahaman, W., Marshall, G. J., Wille, J. D., ... Lachlan-Cope, T. (2019). The Dominant Role of Extreme Precipitation Events in Antarctic Snowfall Variability. *Geophysical Research Letters*, *0*(ja). Retrieved from http://doi.wiley.com/10.1029/2018GL081517 doi: 10.1029/2018GL081517

Vignon, , Roussel, M.-L., Gorodetskaya, I. V., Genthon, C., & Berne, A. (2021, 4). Present and Future of Rainfall in Antarctica. *Geophysical Research Letters*, *48*(8), e2020GL092281. Retrieved from https://doi.org/10.1029/

2020GL092281 doi: https://doi.org/10.1029/2020GL092281

Wille, J. D., Favier, V., Dufour, A., Gorodetskaya, I. V., Turner, J., Agosta, C., & Codron, F. (2019). West Antarctic surface melt triggered by atmospheric rivers. *Nature Geoscience*, *12*(11), 911–916. Retrieved from https://doi.org/10.1038/s41561-019-0460-1 doi: 10.1038/s41561-019-0460-1

Wille, J. D., Favier, V., Gorodetskaya, I. V., Agosta, C., Kittel, C., Beeman, J. C., ... Codron, F. (2021, 4). Antarctic Atmospheric River Climatology and Precipitation Impacts. *Journal of Geophysical Research: Atmospheres*, *126*(8), e2020JD033788. Retrieved from https://doi.org/10.1029/2020JD033788 doi: 10.1029/2020JD033788

Wouters, B., Bamber, J. L., van den Broeke, M. R., Lenaerts, J. T. M., & Sasgen, I. (2013, 8). Limits in detecting acceleration of ice sheet mass loss due to climate variability. *Nature Geoscience*, *6*(8), 613–616. Retrieved from http://www.nature.com/articles/ngeo1874 doi: 10.1038/ngeo1874

Zhu, Y., & Newell, R. E. (1998). A Proposed Algorithm for Moisture Fluxes from Atmospheric Rivers. *Monthly Weather Review*, *126*(3), 725–735. Retrieved from https://journals.ametsoc.org/view/journals/mwre/126/3/1520-0493_1998_126_0725_apafmf_2.0.co_2.xml doi: 10.1175/1520-0493(1998)126⟨0725:APAFMF⟩2.0.CO;2